

---

# Scalable Three-Dimensional Acoustics Using *hp*-finite/infinite Elements and FETI-DP\*

D.K. Datta<sup>1</sup>, S. Dey<sup>1†</sup>, and J.J. Shirron<sup>3</sup>

<sup>1</sup> SFA Inc./NRL, 2200 Defense Dr, Suite 405, Crofton, MD USA 21114. [datta, dey] @pa.nrl.navy.mil † Corresponding author.

<sup>2</sup> Metron Inc., 11911 Freedom Dr, Reston, VA, USA 20190. shirron@metsci.com

**Summary.** This paper addresses scalable, parallel *hp*-finite/infinite element-based solution of time-harmonic acoustics problems in three-dimensions. We discuss the application of FETI-DP, an iterative domain-decomposition scheme, to both interior and exterior acoustics problems. We evaluate parallel scalability in terms of number of iterations, wall-clock time, mesh size  $h$ , polynomial degree  $p$ , number of partitions, and normalized wavenumber. We also discuss the impact of proper selection of the coarse problem on the accuracy of the computed solutions.

## 1 Introduction

Time-harmonic problems in structural acoustics solve *Helmholtz* equation in bounded (interior) and unbounded (exterior) domains. Examples include propagation in bounded waveguides, scattering and radiation from structures in an infinite fluid domain. Numerical solution of such problems in *medium*-frequency regimes with  $p$ -version of finite/infinite elements have been shown to be very effective [DSC01].  $p$ -refinement provides better control of the dispersion (pollution) error enabling increased rate of error convergence compared to  $h$ -refinement.  $hp$ -approximations for three-dimensional problems in structural acoustics, at mid-to-high frequencies, results in large algebraic systems,  $\mathbf{Ax} = \mathbf{b}$ , having millions of unknowns. The efficient solution of such problems calls for the application of scalable parallel algorithms.

Due to the indefinite nature of the algebraic systems coupled with poor conditioning from  $p$ -approximations and frequency-dependence, direct solution techniques have been favoured for such problems. Unfortunately, the parallelization of factorization-based direct solution strategies offer limited scalability due to the high irregularity of matrix factoring. For large-scale problems of our interest, parallel multi-frontal schemes do not scale well beyond 8 processors. A class of domain-decomposition algorithms [SBG96] called FETI-DP

---

\* Research supported by HPCMP.

(see [FLLPR01] and references therein) have been shown to sustain scalability for increasing number of processors.

Most existing research on applying FETI-type algorithms to exterior acoustics problems have used the so-called *artificial boundary conditions* and low-degree  $h$ -approximations [FATL05]. We evaluate FETI-DP applied to 3D acoustics problems discretized by  $p$ -hierarchical finite and infinite elements [DSC01] and highlight the impact of proper selection of the so-called *coarse* problem on solution accuracy.

## 2 Model Problem

Figure 1 shows the computational domain for a typical acoustics problem where  $\Omega_{\pm}$  denotes the exterior/interior fluid domain,  $\Gamma$  denotes the boundary of the obstacle with outward unit normal  $\nu$ , and  $\Gamma_R = \Omega_+ \cap \Omega_-$  is a separable boundary of radius  $R$ . The pressure field  $\phi$  satisfies

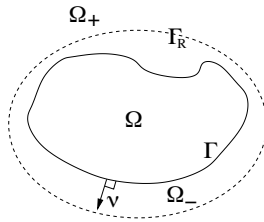


**Fig. 1.** Computational domain.

$$\Delta\phi + k^2\phi = 0 \quad \text{in } \Omega_{\pm}, \quad (1)$$

where  $k = \omega/c$  is the acoustic wavenumber,  $\omega$  is the circular frequency of excitation, and  $c$  is the speed of sound in the fluid. For exterior domains, we consider the Neumann problem with the boundary conditions

$$\frac{\partial\phi}{\partial\nu} = g \quad \text{on } \Gamma, \quad \lim_{r \rightarrow \infty} r \left[ \frac{\partial\phi}{\partial r}(r\hat{e}) - ik\phi(r\hat{e}) \right] = 0 \quad \text{uniformly } \forall |\hat{e}| = 1, \quad (2)$$

where  $g$  is the specified Neumann data and the second equation is the Sommerfeld radiation condition prescribing the out-going asymptotic behavior of  $\phi$ . For problems in which an incident wave  $\phi_0$  scatters from the rigid body enclosed by  $\Gamma$ , we have  $g = -\partial\phi_0/\partial\nu$ . For interior acoustic problems, we apply a Robin boundary condition  $\partial\phi/\partial\nu - ik\phi = h$  on  $\Gamma$ . Both the interior and exterior problems are uniquely solvable for all wavenumbers.

Following standard Galerkin technique results in a weak (variational) form of the interior acoustics problem: Find  $\phi \in H^1(\Omega_-)$  such that

$$\mathcal{B}_-(\phi, \psi) + \mathcal{C}(\phi, \psi) = \mathcal{L}_h(\psi)$$

for all  $\psi \in H^1(\Omega_-)$ , where  $\mathcal{B}_-(\phi, \psi) = \int_{\Omega_-} (\nabla \phi \cdot \nabla \psi - k^2 \phi \psi) d\Omega_-$ ,  $\mathcal{C}(\phi, \psi) = \int_{\Gamma} \psi M \phi d\Gamma$ , and  $\mathcal{L}_h(\psi) = \int_{\Gamma} h \psi d\Gamma$ .

Similarly, for exterior problems, we seek test and trial functions  $\phi, \psi \in H^1(\Omega_-)$ , such that  $\phi = \phi_R$  and  $\psi = \psi_R$  on  $\Gamma_R$ . The functions  $\phi_R$  and  $\psi_R$  with support in  $\Omega_R^+$  satisfy the Sommerfeld radiation condition. Weak form of the exterior problem satisfies

$$\mathcal{B}_-(\phi, \psi) + \mathcal{B}_R(\phi_R, \psi_R) = \mathcal{L}_g(\psi),$$

where  $\mathcal{L}_g(\psi) = \int_{\Gamma} g \psi d\Gamma$ . The bilinear form  $\mathcal{B}_R$  is given by

$$\mathcal{B}_R(\phi_R, \psi_R) = \lim_{S \rightarrow \infty} \left[ \int_{\Omega_{RS}^+} (\nabla \phi_R \cdot \nabla \psi_R - k^2 \phi_R \psi_R) d\Omega_{RS}^+ - ik \int_{\Gamma_S} \phi_R \psi_R d\Gamma_S \right],$$

where  $\Gamma_S$  denotes a separable surface of radius  $S > R$  and  $\Omega_{RS}^+$  is the annular domain bounded by  $\Gamma_R$  and  $\Gamma_S$ .

Let  $\Delta_h^f$  be the spatial discretization of the fluid domain  $\Omega_-$ , with  $h$  representing a measure of the spatial mesh size. Let  $p_f \geq 1$  and  $q_f \geq 0$  be polynomial degrees of finite and radial degree of infinite fluid elements, respectively. Our discrete interior and exterior problems consist of solving

$$\mathcal{B}_-(\phi^{(h, p_f)}, \psi) + \mathcal{C}(\phi^{(h, p_f)}, \psi) = \mathcal{L}_h(\psi) \quad (3)$$

$$\mathcal{B}_-(\phi^{(h, p_f)}, \psi) + \mathcal{B}_R(\phi_R^{(h, p_f, q_f)}, \psi_R) = \mathcal{L}_g(\psi_R), \quad (4)$$

respectively, where  $\phi^{(h, p_f)}$ ,  $\phi_R^{(h, p_f, q_f)}$  belong to a finite-dimensional subset of the admissible space of functions for a given  $h$ ,  $p_f$  and  $q_f$  (see [DSC01]).

### 3 Review of FETI-DP

Let the domain  $\Omega_-$  be subdivided into  $N$  subdomains  $\Omega_s^i, i = 1, \dots, N$ . Each subdomain is discretized using finite elements and we get the system of equations  $K^s u^s = f^s$ , where  $K^s$ ,  $u^s$ , and  $f^s$  are the finite element left-hand side matrix, the solution and the right-hand side load vector, respectively, for  $\Omega_s$ . This can be rewritten as

$$\begin{bmatrix} K_{rr}^s & K_{rc}^s \\ K_{rc}^{sT} & K_{cc}^s \end{bmatrix} \begin{bmatrix} u_r^s \\ u_c^s \end{bmatrix} = \begin{bmatrix} f_r^s \\ f_c^s \end{bmatrix} \quad (5)$$

where the degrees of freedom of a subdomain are divided into two groups  $r$  and  $c$  referred to as the ‘‘interior’’ and ‘‘corner’’ degrees of freedom, respectively. The  $c$  degrees of freedom are created at a global level such that we have  $B_c^{1T} u_c^1 = B_c^{2T} u_c^2 = \dots = B_c^{NT} u_c^N = u_c$ , where  $B_c^s$  maps the corner degrees of

freedom of  $\Omega_s$  to the set of global corner degrees of freedom. The subdomain equations can now be written as

$$\begin{aligned} K_{rr}^s u_r^s + K_{rc}^s B_c^s u_c &= f_r^s \\ \sum_{s=1}^{s=N} B_c^{sT} K_{rc}^s u_r^s + \sum_{s=1}^{s=N} B_c^{sT} K_{cc}^s B_c^s u_c &= \sum_{s=1}^{s=N} B_c^{sT} f_c^s = f_c \end{aligned} \quad (6)$$

At the interfaces of the subdomains, the continuity of subdomain solutions is imposed by the following condition

$$u_b^m - u_b^n = 0 \quad \text{on } \Gamma_{mn} \quad (7)$$

with  $\Gamma_{mn} = \partial\Omega_s^m \cap \partial\Omega_s^n$  for  $m, n = 1, \dots, N$ , and  $m \neq n$ . Note that index  $b$  ( $b \subset r$ ) denotes those degrees of freedom which lie on the interface boundary except the corner degrees of freedom  $c$ . Recasting the above equation as  $\sum_{s=1}^{s=N} B_r^s u_r^s = 0$  where  $B_r^s$  is a signed boolean matrix such that  $B_r^s u_r^s = \pm u_b^s$ , and letting  $\lambda$  denote the lagrange multipliers for enforcing the interface condition (7), leads to the system of equations

$$K_{rr}^s u_r^s + K_{rc}^s B_c^s u_c + B_r^{sT} \lambda = f_r^s, \quad (8)$$

$$\sum_{s=1}^{s=N} B_c^{sT} K_{rc}^s u_r^s + \sum_{s=1}^{s=N} B_c^{sT} K_{cc}^s B_c^s u_c = \sum_{s=1}^{s=N} B_c^{sT} f_c^s = f_c, \quad (9)$$

$$\sum_{s=1}^{s=N} B_r^s u_r^s = 0. \quad (10)$$

Elimination of  $u_r^s$  and  $u_c$  from the above equations gives the interface problem in terms of the dual (lagrange multiplier) solution

$$(F_{rr} + F_{rc} K_{cc}^* {}^{-1} F_{rc} {}^T) \lambda = d_r - F_{rc} K_{cc}^* {}^{-1} f_c^*. \quad (11)$$

Here  $F_{rr} = \sum_{s=1}^{s=N} B_r^s K_{rr}^s {}^{-1} B_r^{sT}$ ,  $F_{rc} = \sum_{s=1}^{s=N} B_r^s K_{rr}^s {}^{-1} K_{rc}^s B_c^s$ ,  $K_{cc}^* = \sum_{s=1}^{s=N} B_c^{sT} K_{cc}^s B_c^s - (K_{rc}^s B_c^s) {}^T K_{rr}^s {}^{-1} K_{rc}^s B_c^s$ ,  $d_r = \sum_{s=1}^{s=N} B_r^s K_{rr}^s {}^{-1} f_r^s$ , and  $f_c^* = f_c - \sum_{s=1}^{s=N} B_c^{sT} K_{rc}^s {}^T K_{rr}^s {}^{-1} f_r^s$ .

In equation (11)  $F_{rr}$  forms a fine-level operator and  $F_{rc} K_{cc}^* {}^{-1} F_{rc} {}^T$  forms a coarse-level operator.

### 3.1 Coarse space for $p$ -approximation and infinite element

Three-dimensional  $p$ -approximations offer multiple options for selecting the ‘‘coarse’’ degrees of freedom. For a partitioned domain, let  $\Sigma = \bigcup_{m,n=1}^N \Gamma_{mn}$ ,  $m \neq n$ , denote the closure of the partition boundary as depicted in Figure

2a. We consider as “coarse” candidates only those subdomain basis functions which have support on mesh entities that belong to the boundary of at least three partitions. This implies that only mesh edges and vertices contribute to the coarse space. If  $M_i^d$  denotes the  $i$ -th mesh entity of dimension  $d$  then Figure 2b depicts the closure of all the candidate mesh entities denoted by  $\Sigma_e$ . Knowing that there are  $p_f - 1$  edge modes in addition to the linear (vertex) modes, suggests two schemes to pick coarse  $dofs$ :

- C1** Consider only vertex modes. No edge modes.
- C2** Consider vertex and edge  $p$ -modes.

Additional care is needed when considering a coarse problem space for an exterior discretization consisting of both finite and infinite elements as shown in Figure 2c. Let  $M_j^3$  be a mesh region in  $\Omega_-$  and let  $M_i^2$  be a corresponding mesh face on the infinite boundary implying  $M_i^2 = \partial M_j^3 \cap \Gamma_R$ . The finite element approximation spaces consist of  $S_{\Omega_-}^p$  - the space of degree  $p$  polynomials associated with closure of mesh region  $M_j^3$ . The infinite element approximation [DSC01] consists of the tensor-product space  $\hat{S}_{\Omega_-}^p \otimes S_{\Omega_+}^q$  where  $\hat{S}_{\Omega_-}^p$  is the subset of  $S_{\Omega_-}^p$  with nonzero support on  $M_j^2$  and  $S_{\Omega_+}^q$  is a space of degree  $q_f + 1$  polynomials in  $1/\rho$  which satisfy the Sommerfeld condition. When selecting the  $dofs$  for the a mesh vertex that lies on the intersection of  $\Gamma_R$  and  $\Sigma_e$ , as depicted in Figure 2d, the additional  $q_f + 1$  radial  $dofs$  must also be included.

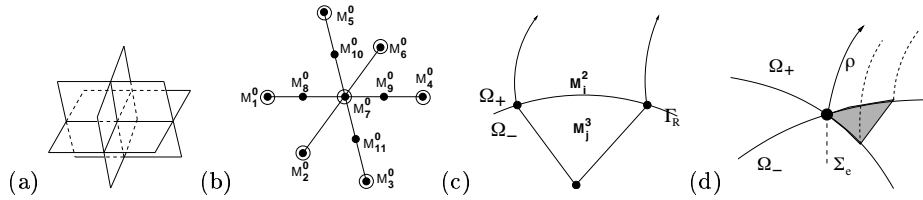


**Fig. 2.** (a) Partition boundary. (b) Closure of mesh entities for coarse problem. (c) Discretization using finite and infinite elements (d) Mesh vertex belonging to infinite element as well as  $\Sigma_e$ .

## 4 Numerical Examples

This section gives several numerical examples to evaluate the performance of FETI-DP for helmholtz problem in 3D for various  $ka$ ,  $p$ , and meshes. In the implementation of FETI-DP within STARS3D, the sub-domain matrices  $K_{rr}^s$  and the coarse problem matrix  $K_{cc}^*$  are assembled in a sparse representation and factored using a sparse multi-frontal solver. For the interface problem (11),

a GMRES based iterative solver [FGGL03] is used with a lumped preconditioner [FLLPR01]. The parallel implementation within STARS3D is based on MPI.

**Interior Helmholtz problem:** Consider the solution of the interior problem in  $\Omega \equiv [-1, -4, -1] \times [1, 4, 1]$  with Robin data  $h = \partial\phi_{\text{ex}}/\partial\nu - ik\phi_{\text{ex}}$ , where  $\phi_{\text{ex}} = \exp(ik|\mathbf{r} - \mathbf{r}_0|)/|\mathbf{r} - \mathbf{r}_0|$  is a point source located at  $\mathbf{r}_0 = (0, -5, 0)$  outside of  $\Omega$ . Three hexahedral meshes, *Mesh A*, *Mesh B* and *Mesh C*, with 8192, 65,536, and 262,144 hexahedrons, respectively, with  $p = 1, 2, 3, 4$  are used. Table 1 gives the iteration counts  $M$ . Table 2 lists the wall-clock

**Table 1.** Iteration counts for interior helmholtz problem for *Mesh A*.

$ka \backslash N$	$p = 1$				$p = 2$				$p = 3$				$p = 4$											
	2	4	8	16	32	64	2	4	8	16	32	64	2	4	8	16	32	64						
10	5	6	4	6	10	9	6	6	5	7	11	12	6	6	5	7	12	13	6	6	5	7	13	16
14	7	7	5	8	12	12	7	8	6	9	15	19	7	8	6	9	17	22	7	8	6	9	20	29
18	7	8	6	10	22	23	9	9	8	11	35	55	9	9	8	11	38	58	9	9	8	11	40	62

**Table 2.** Parallel scalability for interior helmholtz problem with  $ka = 10$ .

$N$	<i>Mesh B</i> , $p = 3$		<i>Mesh B</i> , $p = 4$		<i>Mesh C</i> , $p = 2$		<i>Mesh C</i> , $p = 3$	
	$M$	$Time(Eff.)$	$M$	$Time(Eff.)$	$M$	$STime(Eff.)$	$M$	$Time(Eff.)$
2	6	656.8	6	3346.0	7	3697.0	-	-
4	9	148.2 (221%)	9	631.7 (265%)	9	1061.8 (174%)	9	3849.5
8	8	48.8 (336%)	8	175.4 (477%)	8	298.9 (309%)	9	1375.3 (140%)
32	24	30.2 (136%)	25	75.6 (276%)	25	141.1 (163%)	25	319.9 (154%)

time  $t_N$  and parallel efficiency  $E_N = \frac{Nt_2}{2t_N} \times 100$ . These computations were done on a SGI-Altix. As expected, scalability improves as the problem size grows. Note that *Mesh C*, with  $p = 3$ , has 1.98 million complex degrees of freedom. More than 100% parallel efficiency is observed because of significant drop in total time to factor  $K_{rr}^s$  as the domain is divided into subdomains.

**Exterior Helmholtz problem:** This example considers scattering of plane wave by a rigid obstacle. The incident-wave  $\phi_0$  is along  $(0, 0, -1)$ . Two different shapes for the obstacle are considered: (1) a sphere of radius  $a$ , and (2) a submarine-like structure. The sphere mesh is partitioned based on the coordinate planes, while the mock-submarine (shown in Figure 3) is partitioned using *METIS* ([www-users.cs.umn.edu/~karypis/metis/](http://www-users.cs.umn.edu/~karypis/metis/)).

Table 3 gives the iteration counts for the sphere problem for a mesh with 7896 mesh regions. Here, *unconjugated* infinite elements with radial degree  $q_f = 2$  were used. Similar results for the mock-submarine are given in Table 4.

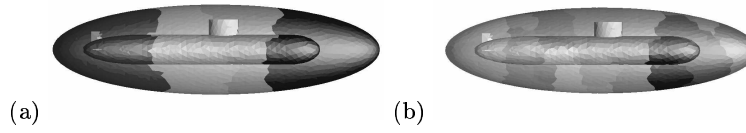


**Fig. 3.** Partitions for mock-submarine. (a)  $N = 4$ , (b)  $N = 32$ .

**Table 3.** Iteration counts for the sphere problem.

		$p = 1$			$p = 2$			$p = 3$			$p = 4$		
$ka \setminus N$	$N$	2	4	8	2	4	8	2	4	8	2	4	8
5		13	5	3	15	6	7	16	7	7	12	8	10
10		16	5	3	21	7	7	20	8	7	12	9	11

**Table 4.** Iteration counts for exterior scattering from a rigid mock submarine. *Mesh*  $H_1$  (*Mesh*  $H_2$ ) has 19024 (60819) regions.

		<i>Mesh</i> $H_1, p = 1$			<i>Mesh</i> $H_2, p = 1$			<i>Mesh</i> $H_1, p = 2$			<i>Mesh</i> $H_2, p = 2$		
$N \setminus ka$	$ka$	1	5	10	1	5	10	1	5	10	1	5	10
4		19	64	415	20	40	162	24	121	236	23	93	386
8		21	93	771	21	67	272	26	190	383	24	140	863
16		21	132	2457	22	92	347	27	243	970	28	169	1403
32		22	153	1906	22	68	716	31	293	2480	30	126	2955

**Impact of coarse problem selection** To evaluate the impact of the choice of method to select the *degrees of freedom* for the *coarse* problem outlined in Section 3.1, we consider the sphere problem. Consider a finite element approximation with  $p_f = 3$  and infinite element radial degree  $q_f = 2$ . We compare the number of iterations needed to converge to a given tolerance. The impact on the accuracy is evaluated by computing the pointwise maximum ( $L_\infty$ ) relative error in the real and the imaginary parts of the computed scattered field as:

$$|\Re(e)|_\infty = \frac{\max_i |\Re(u_i) - \Re(u_i^0)|}{\max_i |\Re(u_i^0)|}, \quad |\Im(e)|_\infty = \frac{\max_i |\Im(u_i) - \Im(u_i^0)|}{\max_i |\Im(u_i^0)|} \quad (12)$$

where,  $u^0$  is a globally  $C^0$  solution obtained by a direct multi-frontal scheme.

From Table 5 we note that use of all the edge modes from  $\Sigma_e$  (**C2**) makes the approximate FETI-DP solution to converge to the globally  $C^0$  solution within the tolerance used in the iterative solution of the interface problem 11. In contrast, use of only vertex (linear) modes (**C1**) make the FETI-DP solution to have errors that significantly exceed the convergence tolerance used in the iterative solver.

**Table 5.** Impact of coarse space selection on iteration counts and accuracy for scattering from rigid sphere at  $ka = 1, 10$ . Lumped preconditioner and a tolerance  $1.0e - 09$  is used for iterative solve.  $n_c$  denotes the number of coarse *dofs*.

	$N = 4$			$N = 8$		
	$M (n_c)$	$ \Re(e) _\infty$	$ \Im(e) _\infty$	$M (n_c)$	$ \Re(e) _\infty$	$ \Im(e) _\infty$
$ka = 1, \mathbf{C1}$	40 (16)	8.34e-3	3.71e-3	40 (48)	8.33e-3	6.21e-3
$ka = 1, \mathbf{C2}$	40 (36)	2.83e-8	1.54e-8	37 (108)	9.13e-9	9.75e-9
$ka = 10, \mathbf{C1}$	100 (16)	1.26e-2	1.59e-2	110 (48)	2.64e-2	2.38e-2
$ka = 10, \mathbf{C2}$	100 (36)	9.08e-9	1.11e-8	102 (108)	8.73e-9	8.31e-9

## 5 Discussion and Conclusion

We have successfully applied the FETI-DP algorithm to *hp*-finite/infinite element discretization of both interior and exterior acoustics problems. We show super-linear scalability for a set of interior acoustics problems. For exterior problems, we demonstrate excellent scalability of FETI-DP except at very high  $ka$  values. The lack of better scalability at higher wavenumber is tied to numerically dispersive nature of these approximations and will be addressed with effective augmentation strategies that accelerate convergence further. We have also discussed strategies for selecting the *coarse* problem space and show that for  $p$ -approximations it is imperative to include all the high-order mesh edge modes to ensure expected accuracy of the subdomain solutions.

## References

- [SBG96] Smith B., Bjørstad P. and Gropp W.: *Domain decomposition: parallel multilevel methods for elliptic partial differential equations*, Cambridge Univ. Press, (1996)
- [FLLPR01] Farhat, C., Lesoinne, M., LeTellec, P., Pierson, K., Rixen, D.: FETI-DP: a dual-primal unified FETI method- part-I: a faster alternative to the two level FETI method. *Int. J. Num. Meth. Engg.*, **50**, 1523–1544 (2001)
- [DSC01] Dey, S., Shirron, J.J., Couchman, L.S.: Mid-frequency structural acoustic and vibration analysis in arbitrary, curved, three-dimensional domains. *Computers and Structures*, **79**, 617–629 (2001)
- [FGGL03] Frayss, V., Giraud, L., Gratton, S., Langou, J.: A set of GMRES routines for real and complex arithmetics on high performance computers. CERFACS Technical Report TR/PA/03/3, (2003) [www.cerfacs.fr/algor/Softs](http://www.cerfacs.fr/algor/Softs).
- [FATL05] Farhat, C., Avery, P., Tezaur, R., Li, J.: FETI-DPH: a dual-primal domain decomposition method for acoustic scattering. *J. Comp. Acoustics.*, *To appear*, (2005)